

# NJC

Accepted Manuscript



This article can be cited before page numbers have been issued, to do this please use: X. Guo, J. Zhang, Y. Cui, S. Chen, H. Sun, Q. Yang, G. Ma, L. Wang and J. Kang, *New J. Chem.*, 2019, DOI: 10.1039/C9NJ00950G.



This is an Accepted Manuscript, which has been through the Royal Society of Chemistry peer review process and has been accepted for publication.

Accepted Manuscripts are published online shortly after acceptance, before technical editing, formatting and proof reading. Using this free service, authors can make their results available to the community, in citable form, before we publish the edited article. We will replace this Accepted Manuscript with the edited and formatted Advance Article as soon as it is available.

You can find more information about Accepted Manuscripts in the [author guidelines](#).

Please note that technical editing may introduce minor changes to the text and/or graphics, which may alter content. The journal's standard [Terms & Conditions](#) and the ethical guidelines, outlined in our [author and reviewer resource centre](#), still apply. In no event shall the Royal Society of Chemistry be held responsible for any errors or omissions in this Accepted Manuscript or any consequences arising from the use of any information it contains.

## ARTICLE

## Highly biocompatible jujube polysaccharide-stabilized palladium nanoparticles with excellent catalytic performance

Xiaolei Guo<sup>a</sup>, Jin Zhang<sup>b</sup>, Yanshuai Cui<sup>\*a</sup>, Shengfu Chen<sup>c</sup>, Haotian Sun<sup>c</sup>, Qinghua Yang<sup>d</sup>, Guanglong Ma<sup>c</sup>, Longgang Wang<sup>\*a</sup>, Jianxin Kang<sup>a</sup>

The development of stable and biocompatible palladium nanoparticles (Pd NPs) catalysts has been drawing great interest. In this study, Pd NPs were prepared through a green method, where jujube polysaccharide (JP) was employed as both reducing and stabilizing agents for the first time. The JP stabilized palladium nanoparticles (Pd<sub>n</sub>-JP NPs) displayed small size, high stability, good biocompatibility and excellent catalytic efficiency. Pd<sub>50</sub>-JP NPs showed high stability up to two weeks in solutions of wide pH range (4 - 9). Pd<sub>50</sub>-JP NPs showed negligible cytotoxicity against HeLa cells at high concentration up to 400 µg/mL. Furthermore, Pd<sub>n</sub>-JP NPs showed excellent catalytic activity for reduction of 4-nitrophenol (4-NP) in the presence of sodium borohydride (NaBH<sub>4</sub>). The normalized rate constant ( $k_{nor}$ ) and turnover frequency (TOF) of Pd<sub>50</sub>-JP NPs were as high as 38.4 s<sup>-1</sup>mM<sup>-1</sup> and 4455 h<sup>-1</sup>, respectively. The prepared Pd<sub>n</sub>-JP NPs have various potential applications in bio-related catalysis in the future.

### 1 Introduction

Nitro-containing compounds are common organic pollutants in the water. They are extremely harmful to the environment and human health.<sup>1,2</sup> Among them, 4-NP is a kind of highly toxic and refractory organic pollutant. However, 4-aminophenol (4-AP) is an important chemical intermediate. It has been widely used in development of pesticides, pharmaceuticals, dyes and leather.<sup>3,4</sup> Therefore, generation of 4-AP from 4-NP is important for environmental protection and resources regeneration.<sup>5,6</sup> This is in line with the green chemical concept.<sup>7</sup> At present, various materials including metal nanoparticles,<sup>8,9</sup> metal oxide nanoparticles and metal nanoparticle-decorated 2D materials<sup>10-12</sup> have been studied in this reduction reaction in the presence of NaBH<sub>4</sub>. It is generally believed that the mechanism of this reaction follows the Langmuir-Hinshelwood kinetics.<sup>13,14</sup> However, the commonly used method for synthesis of noble metal nanoparticles has many disadvantages such as strict conditions, toxic solvents and harmful by-products.<sup>15</sup> Therefore, exploring environmentally friendly method to prepare noble metal nanoparticle has gradually become a research hotspot in

the field of nanocatalyst synthesis.<sup>16</sup>

Green synthesis of nanoparticles is an environmentally friendly, low energy and low cost method. Various microorganisms including fungi,<sup>17</sup> bacteria<sup>18</sup> and plant extracts<sup>19</sup> have been widely used for green synthesis of metal nanoparticles. Among them, the plants extracts has become popular raw material in recent years due to the easy access.<sup>20</sup> Mahmoud and co-workers used the extract from leaves of Euphorbia esula L. to synthesize Cu NPs with a particle size of less than 32 nm and a non-uniform morphology.<sup>21</sup> MubarakAli and co-workers used extract of the Mentha piperita to synthesize Au NPs around 150 nm.<sup>22</sup> However, plant extracts are rich in various components such as proteins, pigments and polysaccharide. It is usually difficult for reproducibility of morphology and sizes of nanoparticles resulting from the uncertain composition. Yu and co-workers synthesized Au NPs by Citrus maxima water extract and studied their catalytic reduction of 4-NP performance.<sup>23</sup> The  $k_{app}$  is only 0.08977 min<sup>-1</sup> at a catalyst concentration of 1 mmol/L, which is lower compared with that in many reports. The low catalytic activity of NPs may be attributed to their low stability in water. Thus, it is necessary to isolate the plant extracts to obtain soluble macromolecules with reducing power. Natural polysaccharide meet the above criteria and are rich in plant. Moreover, polysaccharide eliminate oxygen free radicals, which gives them wide application such as improving immunity,<sup>24</sup> anti-tumor, anti-virus,<sup>25</sup> anti-aging, anti-infection and anti-ulcer.<sup>26</sup> In addition, polysaccharide form an independent space at the molecular level due to the interaction of their hydrogen bonds, which may serve as good templates for the growth of nano-ions. JP has good biocompatibility, biodegradability and high molecular weight. Jujube is a kind of healthy food with nutritional value and medicinal value. It is also widely distributed and easy to obtain at a low price.

<sup>a</sup> Key Laboratory of Applied Chemistry, College of Environmental and Chemical Engineering, Yanshan University, Qinhuangdao, 066004, China.

<sup>b</sup> College of Chemistry and Environmental Engineering, Shanxi Datong University, Datong, 037009, China.

<sup>c</sup> Key Laboratory of Biomass Chemical Engineering of Ministry of Education, College of Chemical and Biological Engineering, Zhejiang University, Hangzhou, 310027, China.

<sup>d</sup> School of Medical Engineering Hefei University of Technology, Hefei, 230009, China.

Pd NPs have been found to be catalytically active in aqueous solution, in cell culture and *in vivo*.<sup>27,28</sup> They have higher catalytic ability in reduction of 4-NP compared with Pt NPs and Au NPs.<sup>29</sup> Here, we proposed a green method, in which Pd<sub>n</sub>-JP NPs were prepared using JP as stabilizer and reducing agent. To the best of our knowledge, there is no report on the synthesis of Pd NPs from JP. The Pd<sub>n</sub>-JP NPs had small size and narrow size distribution for Pd NPs. The stability of Pd<sub>n</sub>-JP NPs in solutions with different pH values and toxicity against cells and bacteria were carefully studied. More importantly, the catalytic activity of Pd<sub>n</sub>-JP NPs was evaluated in reduction of 4-NP by NaBH<sub>4</sub>. The results revealed that Pd-JP NPs are highly stable, biocompatible and efficient as catalysts.

## 2 Materials and methods

### 2.1. Materials

Sodium tetrachloropalladate (Na<sub>2</sub>PdCl<sub>4</sub>), NaBH<sub>4</sub>, hydrogen peroxide (H<sub>2</sub>O<sub>2</sub>), trichloromethane, butyl alcohol, potassium ferricyanide, trichloroacetic acid, iron(III) chloride hexahydrate, sodium chloride, potassium chloride, dibasic sodium phosphate, potassium phosphate monobasic, 3-(4,5)-dimethylthiaziazolo(-z-y1)-3,5-diphenyltetrazoliumromide (MTT) and 4-NP were purchased from Aladdin. Jujube was purchased from a local supermarket. All cell lines were purchased from China Center for Typical Culture Collection.

### 2.2 Extraction of JP

Dried jujube powder samples were extracted with water at 70 °C (1:15 (w/v), 3 h, twice).<sup>30,31</sup> The water extraction solution was obtained by centrifugation, and pigment was removed by the addition of H<sub>2</sub>O<sub>2</sub> at 50 °C (1:15 (v/v), 1.5 h). The resulting solution was mixed with sewage reagent (5:1 (v/v)) and centrifuged to remove proteins. The sewage reagent was composed of chloroform and butyl alcohol (5:1 (v/v)). The generated solution was freeze-dried to obtain JP.<sup>32</sup>

### 2.3 Determination of reducing power of JP

The reducing power of JP was determined according to the previous report with slight changes.<sup>33</sup> 1.0 mL of JP aqueous solution with different concentration (0.0625~2 mg/mL), 2.5 mL of phosphate buffer saline (PBS) at pH=6.6, and 2.5 mL of potassium ferricyanide solution with a mass fraction of 1% were added, respectively. The mixed solution was rapidly cooled down after being kept in a water bath at 50 °C for 20 minutes. 2.5 mL of 10% trichloroacetic acid solution was added. After centrifuging the mixed liquid, 2.5 mL of the supernatant was collected and added into a 10 ml centrifuge tube, and 2.5 mL of distilled water and 0.5 mL of 0.1% ferric chloride solution were sequentially added. 10 min later, the absorbance of the solution at 700 nm was measured.

### 2.4 Preparation of JP stabilized Pd<sub>n</sub>-JP NPs

Pd<sub>n</sub>-JP NPs were prepared by using Na<sub>2</sub>PdCl<sub>4</sub> as a metal source and JP as reducing agent. Briefly, JP aqueous solution was mixed with 1 mM Na<sub>2</sub>PdCl<sub>4</sub>, where the molar ratio of Na<sub>2</sub>PdCl<sub>4</sub> to JP was 50, 100, and 200, respectively. The solutions were incubated for 4 h, and the color of the solution changed from light yellow to brown.

### 2.5 Size and zeta potential measurements

View Article Online

DOI: 10.1039/C9NJ00950G

The size and zeta potential measurements of the Pd<sub>n</sub>-JP NPs were determined using dynamic light scattering (DLS) technology with a Zetasizer Nano ZS system (Malvern, UK). 100 µL of 5 mg/mL Pd<sub>50</sub>-JP NPs were dissolved in 900 µL of PBS with different pH (4, 5, 6, 7, 8 or 9), respectively. Each sample had triplicate and was measured at 25 °C. The sizes of the Pd NPs were characterized by HT7700 transmission electron microscopy (TEM) operating at 100 kV in bright field mode.

### 2.6 Biocompatibility

Cell viability assay was performed according to the previous reports.<sup>34,35</sup> HeLa cells were seeded in 96-well cell culture plates at 10<sup>4</sup> cells/well. The cells were cultured in an incubator at 37 °C and CO<sub>2</sub> concentration of 5%. After 24 h, the original high-glucose DMEM medium with 10% FBS was replaced by different concentrations of Pd<sub>50</sub>-JP NPs medium. Each group had 3 replicate wells. The medium was removed after 24 h, and 100 µL of 0.5 mg/mL MTT solution was added. After 4 h, the MTT culture medium was replaced by 150 µL of DMSO. The culture plates were shaken for 10 min. The absorbance of the samples at 490 nm was measured by a microplate reader. Cell viability assay was calculated by comparison the absorbance of samples with that of control groups.

Cellular uptake assay was performed according to the previous reports.<sup>36,37</sup> HeLa cells (5×10<sup>4</sup> cells/well) were seeded in 24-well cell culture plates. After 24 h of culture, the original medium was replaced by a medium solution of 400 µg/mL Pd<sub>50</sub>-JP NPs. After 24 h, the medium was removed, and the cells were washed with PBS and digested with trypsin. The cells were collected by centrifugation and washed with PBS. 1 mL of 10% HNO<sub>3</sub> was added, the mixture was allowed to stand at 80 °C overnight. After diluting 10 times on the next day, the palladium concentration was measured by ICP-MS.

Bacterial toxicity assay was performed according to the previous reports.<sup>38</sup> The bacterial toxicity of Pd<sub>n</sub>-JP NPs was studied using Escherichia coli (E. coli, gram-negative bacterium) and Staphylococcus aureus (S. aureus, gram-positive bacterium). E.coli and S.aureus colonies were added into nutrient broth (NB). They were both cultured overnight at 37 °C with 150 r/min. The next day, 90 µL of bacterial culture (10<sup>7</sup> CFU/mL) was added into a 96-well culture plate. 10 µL of Pd<sub>100</sub>-JP NPs ranging concentration from 300 to 1200 µg/mL were added to each well. Bacteria were cultured at 37 °C and 50 r/min for 24 h. The absorbance value of each well was measured at 600 nm by a microplate reader.

### 2.7 Catalytic activity

(a) Catalytic reduction of 4-NP: 250 µL of 0.6 mM 4-NP and 650 µL of deionized water were mixed in a cuvette. Then, 100 µL of 20 nM Pd<sub>50</sub>-JP and 1 mL of 0.5 M fresh NaBH<sub>4</sub> solution were added. The reaction system was monitored every 3 min using an UV-Vis spectrophotometer.

(b) In situ detection of 4-NP reduction: 200 µL of 0.6 mM 4-NP aqueous solution and deionized water (750 µL, 700 µL or 650 µL) were mixed in a cuvette, respectively. Then, 50 µL, 100 µL or 150 µL of 20 nM Pd<sub>n</sub>-JP and 1 mL 0.5 M of fresh NaBH<sub>4</sub> solution were

added. The absorbance at 400 nm was monitored by UV-Vis spectrophotometer.

## 3 Results and discussion

### 3.1. Reducing power of JP

JP is a kind of natural biomacromolecule with aldehyde groups, hydroxyl groups and ketone groups, which determine its solubility and reducing power. This property makes it possible to stabilize and reduce metal nanoparticles. Here, the reducing power of JP was measured by reducing  $\text{Fe}^{3+}$ . In the reduction power measurement, the antioxidant reduced  $\text{Fe}^{3+}$  to generate  $\text{Fe}^{2+}$  by providing electrons. The formation of  $\text{Fe}^{2+}$  could be monitored by measuring the absorbance at 700 nm.<sup>39</sup> Thus, the reducing power was linear with the absorbance. Fig. 1 showed that the reducing power of JP was positive correlation with its concentration. The absorbance of JP was 0.25 at concentration of 2.0 mg/ml. This reducing power of JP makes it an antioxidant and anti-aging healthcare product.<sup>40</sup>

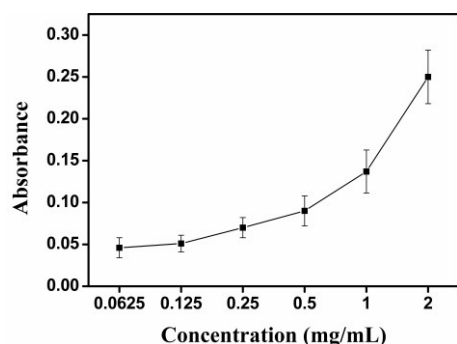


**Fig. 1** UV-Vis absorbance at 700 nm with different concentrations of JP. The result indicated that the reducing power of JP was positive correlation with its concentration.

### 3.2. Pd<sub>n</sub>-JP NPs synthesis and characterization

As has been demonstrated, JP had reducing power, which might be used to reduce  $\text{PdCl}_4^{2-}$  to generate zero-valent Pd NPs without using additional reducing agent. The JP and  $\text{Na}_2\text{PdCl}_4$  were mixed together and incubated for 4 h. Fig. 2a showed that the color of the prepared Pd<sub>n</sub>-JP NPs solution was gradually deepened as the molar ratio of  $\text{Na}_2\text{PdCl}_4$  to JP increased. In addition, Fig. 2b showed the spectra of Pd<sub>n</sub>-JP, JP, and  $\text{Na}_2\text{PdCl}_4$ . The absorption peak at 235 nm was assigned to  $\text{Na}_2\text{PdCl}_4$ . After the mixed reaction with JP, the disappearance of the peak at 235 nm indicated that Pd(II) was reduced to Pd(0).<sup>41,42</sup> In addition, the color of the solution changed from light yellow to brown, which also proved the presence of Pd(0). Both results indicated the formation of Pd<sub>n</sub>-JP NPs. In short, the Pd<sub>n</sub>-JP NPs were prepared using JP as a green synthetic method.

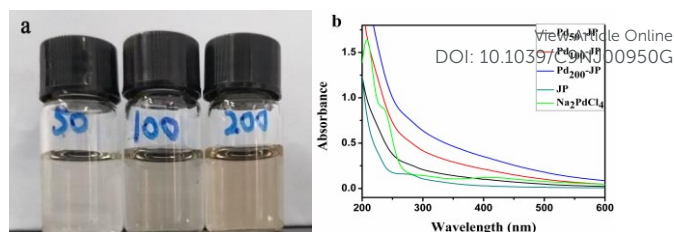


**Fig. 2** (a) The photos of Pd<sub>n</sub>-JP solution (n=50, 100, 200). (b) UV-Vis spectra of Pd<sub>n</sub>-JP (2 μM), JP (2 μM), and  $\text{Na}_2\text{PdCl}_4$  (200 μM). The results indicated the successful preparation of Pd<sub>n</sub>-JP NPs.

Furthermore, the JP and Pd<sub>100</sub>-JP NPs were measured by using FTIR spectra. As illustrated in Fig. 3, in the JP spectrum, the absorption peaks at 3430  $\text{cm}^{-1}$  and 2935  $\text{cm}^{-1}$  were caused by the strong stretching vibration of O-H and C-H, respectively. The peaks at 1740 and 1630  $\text{cm}^{-1}$  were attributed to stretching vibrations and asymmetric stretching vibration of C=O. The peaks at 1100 and 1020  $\text{cm}^{-1}$  were due to C-OH tensile vibration. In the spectrum of Pd<sub>100</sub>-JP NPs, the absorption peak at 1740  $\text{cm}^{-1}$  was weaker than that of JP, which indicated that the interaction between Pd NPs and the carbonyl group of JP. In addition, the intensity of the two peaks at 1100 and 1020  $\text{cm}^{-1}$  also significantly was reduced, which should be attributed to the interaction of Pd NPs with C-OH from the polysaccharide. Hence, the interaction between the resulting Pd NPs and various groups of JP can result in the position and intensity change of transmittance peak in the FTIR spectra of JP and Pd<sub>100</sub>-JP NPs.<sup>43,44</sup>

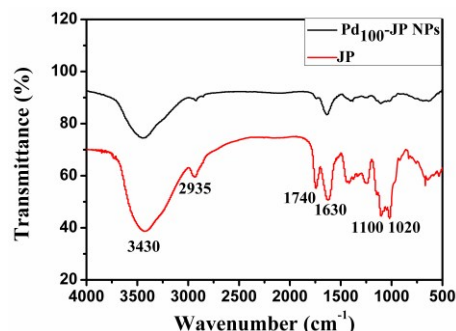


**Fig. 3** FTIR spectra of JP and Pd<sub>100</sub>-JP NPs. The result indicated that there was interaction between the Pd NPs and groups of JP.

When nanoparticles are used as catalysts, the relatively narrow size dispersion and small particle size generally enhance their catalytic ability. Small nanoparticles exhibit high specific surface area, providing more access opportunities for substrate. The size of Pd NPs was measured by using TEM. As shown in Fig. 4, Pd NPs were spherical and monodispersed. The calculated average diameters of Pd NPs were  $5.71 \pm 1.62$  nm for Pd<sub>50</sub>-JP;  $6.07 \pm 1.84$  nm for Pd<sub>100</sub>-JP;  $6.17 \pm 1.36$  nm for Pd<sub>200</sub>-JP, respectively. Thus, small Pd NPs particle size (5-7 nm) indicated that Pd<sub>n</sub>-JP NPs had a large specific surface area. This provided more active sites to enhance catalytic performance during the catalytic reaction.

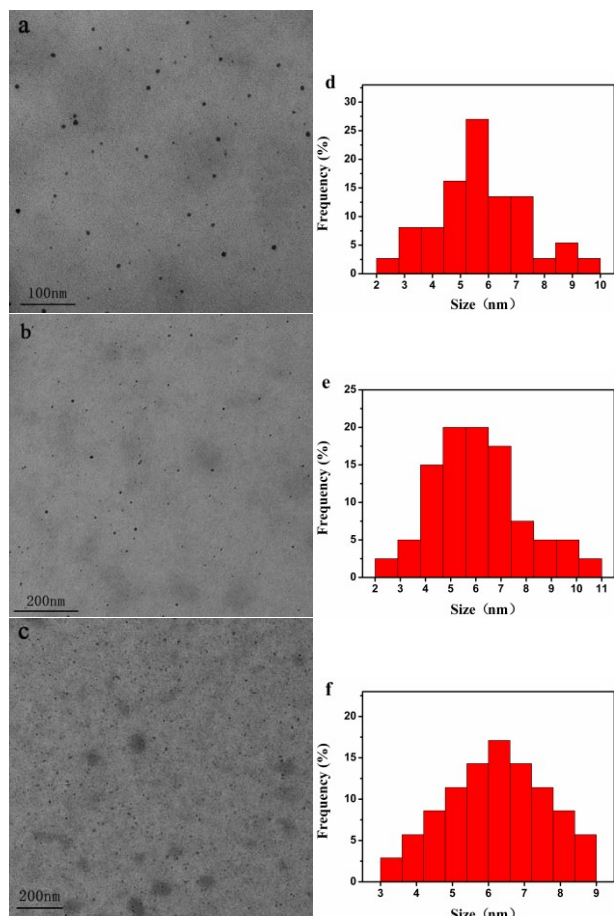


**Fig. 4** TEM images and size distribution histograms of (a,d) Pd<sub>50</sub>-JP NPs, (b,e) Pd<sub>100</sub>-JP NPs, (c,f) Pd<sub>200</sub>-JP NPs. The average sizes of Pd NPs were  $5.71 \pm 1.62$  nm for Pd<sub>50</sub>-JP;  $6.07 \pm 1.84$  nm for Pd<sub>100</sub>-JP;  $6.17 \pm 1.36$  nm for Pd<sub>200</sub>-JP, respectively. The results indicated that Pd NPs had small size and narrow size distribution.

### 3.3 Stability

Catalytic degradation of organic pollutants is usually carried out in water. Good dispersion of nanoparticles without aggregation under various conditions is beneficial to their high catalytic performance. Here, the stability of Pd<sub>50</sub>-JP NPs was evaluated as an example through the change of their hydrodynamic size. The hydrodynamic size of Pd<sub>50</sub>-JP NPs in PBS with different pH was measured using DLS. As shown in Fig. 5a, the hydrodynamic size of Pd<sub>50</sub>-JP NPs was about 30 nm in the pH range of 4-9 after 24 h. In addition, after 2 weeks, there was no significant change of the hydrodynamic size of Pd<sub>50</sub>-JP NPs. Thus, Pd<sub>n</sub>-JP NPs had excellent stability in different pH solutions for a long time. As for Pd<sub>50</sub>-JP NPs, the hydrodynamic size value measured by DLS was larger than the size measured by TEM, which was because the sample measured by DLS contained the JP template with hydrated states, while size measured by TEM was Pd NPs with dried states. The zeta potential of Pd<sub>50</sub>-JP NPs was also measured. As shown in Fig. 5b, the zeta potential of Pd<sub>50</sub>-JP NPs was in the range from -0.19 to -1.53 mV. This indicated that there was weak electrostatic repulsion between the Pd<sub>n</sub>-JP NPs. This prevented mutual attraction or aggregation of Pd<sub>n</sub>-JP NPs in solution to some extent.<sup>45,46</sup> In short, the Pd<sub>n</sub>-JP NPs displayed excellent stability in different pH buffer solutions, showing their potential catalytic application in a wide pH range solution.

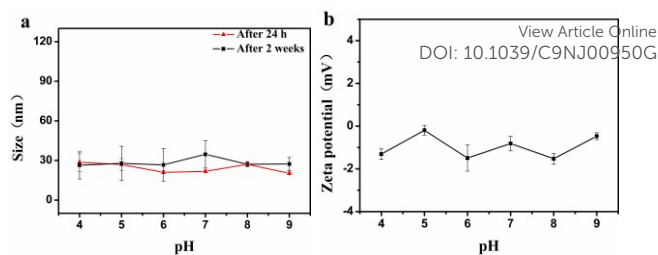


**Fig. 5** The stability (a) and zeta potential (b) of Pd<sub>50</sub>-JP NPs under different pH. The Pd<sub>50</sub>-JP NPs displayed excellent stability from pH 4 to 9 within 2 weeks and low net charge. The results indicated that the high stability of Pd<sub>50</sub>-JP NPs was attributed to the presence of JP.

### 3.4 Biocompatibility

When organic pollutants are catalytically degraded in the nature, the sewage contains a large amount of microorganisms. The strong interaction between nanoparticles and microorganisms often leads to high toxicity and reduced catalytic performance. For example, the generation 5 poly(amido amine) dendrimers encapsulated Pd NPs (Pd<sub>55</sub>-G5 NPs) have high toxicity against cells and bacteria.<sup>47</sup> Here, the toxicity of Pd<sub>n</sub>-JP NPs was assessed. Two models (HeLa cells and bacteria) were incubated with Pd<sub>n</sub>-JP NPs. The cytotoxicity of Pd<sub>n</sub>-JP NPs was evaluated by MTT assay *in vitro*.<sup>48</sup> Fig. 6a showed that the cell viability of Pd<sub>50</sub>-JP NPs and JP was > 90% within 400 μg/mL. In addition, the cytotoxicity of Pd<sub>50</sub>-JP NPs was evaluated by observing the morphology of HeLa cells. Fig. 6b showed the HeLa cell morphology of the control group after 24 h. HeLa cells incubated with Pd<sub>50</sub>-JP NPs and JP had similar morphology with the control groups. Taken together, these results indicated that Pd<sub>50</sub>-JP NPs displayed very good cytocompatibility. In order to study the mechanism of high cytocompatibility, the cellular uptake of Pd<sub>50</sub>-JP NPs was determined by ICP-MS. Here, the cellular uptake of Pd<sub>50</sub>-JP NPs was 1.98 ng/10<sup>4</sup> cells. As shown in Fig. 6c, the cellular uptake of Pd<sub>50</sub>-JP NPs was a little higher than that of control group, while the cellular uptake of Pd<sub>55</sub>-G5 NPs was 12 to 13 times that of Pd<sub>50</sub>-JP NPs.<sup>47</sup> The results indicated that Pd<sub>50</sub>-JP NPs showed little accumulation in HeLa cells. This was attributed to the natural green JP template and the negative charge of the Pd<sub>50</sub>-JP NPs surface, limiting the entry of Pd<sub>50</sub>-JP NPs into the cell. However, Pd<sub>55</sub>-G5 NPs have highly positive charge on their surface, resulting in their high accumulation in HeLa cells and high cytotoxicity.

In addition, the bacterial viability of Pd<sub>100</sub>-JP NPs was detected by incubating them with the bacteria (*E.coli* and *S.aureus*) in NB for 24 hours. Bacterial viability was defined as comparison the optical density of samples with the control groups at 600 nm. Fig. 6d shows bacterial viabilities of *E.coli* and *S.aureus* were ≥ 96.6%. The results indicated that Pd<sub>50</sub>-JP did not suppress the growth of both bacteria. To sum up, Pd<sub>50</sub>-JP NPs had very good biocompatibility *in vitro*. The high biocompatibility exhibited by Pd<sub>50</sub>-JP NPs should be attributed to the JP template. The high biocompatibility of Pd<sub>50</sub>-JP NPs was beneficial to make them environmentally friendly catalyst for bio-related catalytic applications.

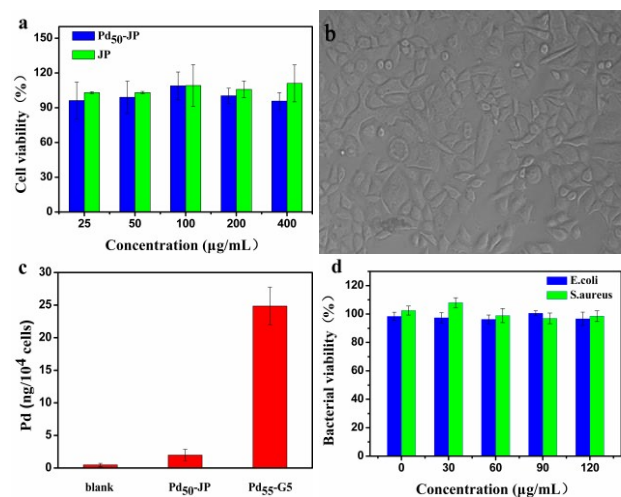


**Fig. 6** (a) Cell viabilities of HeLa cells for Pd<sub>50</sub>-JP NPs and JP. (b) Cell morphology of the HeLa cells for the control group. (c) ICP-MS measurements for Pd contents. (d) The relationship between bacterial viability and the concentrations of Pd<sub>100</sub>-JP NPs in NB after incubation with *E. coli* and *S. aureus* for 24 hours. The results indicated the high cell viability was due to the low cellular uptake of Pd<sub>50</sub>-JP NPs. Pd<sub>100</sub>-JP NPs did not suppress the growth of bacterial.

### 3.5 Catalytic efficiency

As described above, Pd<sub>n</sub>-JP NPs were synthesized by a green method. They were small, monodisperse, stable and biocompatible *in vitro*. Furthermore, the catalytic activity of Pd<sub>n</sub>-JP NPs was investigated using catalytic reduction of 4-NP as a model. 4-NP is mainly derived from common pollutants in industry and agriculture. If 4-NP is directly discharged into the water, it will cause serious pollution to the environment.<sup>49</sup> Therefore, it is necessary to treat the 4-NP of wastewater. It has been reported that the 4-NP can be reduced to useful 4-AP by using the Pd NPs. Here, the catalytic properties of Pd<sub>n</sub>-JP were investigated by the reduction of 4-NP in the presence of excess of NaBH<sub>4</sub>. As shown in Fig. 7a, 4-NP had an absorption peak at 312 nm. After adding NaBH<sub>4</sub>, the mixed solution had maximal absorption peak at 400 nm, which corresponds to new generated 4-hydroxyaminophenol (4-Hx).<sup>50</sup> The color of the 4-NP solution changed from pale yellow to deep yellow. As shown in Fig. 7b, after the addition of Pd<sub>n</sub>-JP, the intensity of the absorption peak at 400 nm decreased with increasing time. At the same time, a new absorption peak at 295 nm appears, which indicated the formation of the reduced product of 4-AP.<sup>1,51</sup> About 18 min later, the color of this solution became colorless. On the contrary, the reduction of the 4-NP without the catalyst was very slow, and the absorbance at 400 nm decreased only 15% after 210 minutes. The reduction of 4-NP by NaBH<sub>4</sub> and JP has been carried out. The absorbance at 400 nm did not decrease over 12 minutes, indicated that the intermediate 4-Hx did not react to give the final product 4-AP. JP only acted as a stabilizer for Pd NPs and did not participate in the catalytic process, while Pd NPs were the catalytic center. The increase in 4-NP reduction is due to the presence of Pd<sub>n</sub>-JP. Pd<sub>n</sub>-JP could enhance electrons transfer from BH<sub>4</sub><sup>-</sup> ions to 4-NP nitro groups.<sup>52</sup>

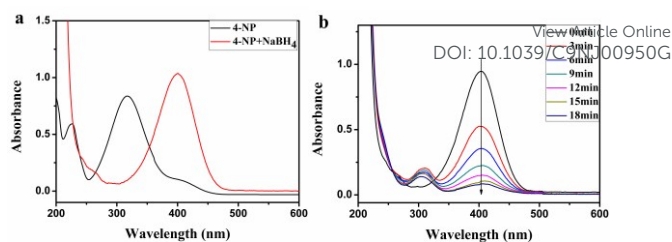
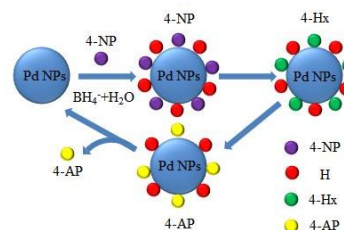


**Fig. 7** (a) The UV-Vis spectra of 4-NP and 4-NP+NaBH<sub>4</sub>. (b) The UV-Vis spectra of the reduction of 4-NP using Pd<sub>50</sub>-JP NPs every 3 min. The results indicated that 4-NP was quickly reduced to 4-AP using Pd<sub>50</sub>-JP NPs with NaBH<sub>4</sub>.



**Scheme 1** Schematic representation of catalytic reduction of 4-NP by Pd NPs in the presence of NaBH<sub>4</sub>.<sup>7</sup>

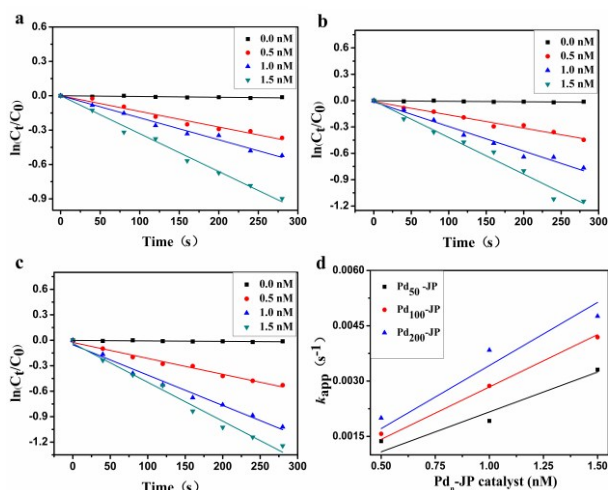
The mechanism of reduction of 4-NP catalyzed by noble metal nanoparticles has been reported by many groups.<sup>14,53</sup> This reaction should follow Langmuir-Hinshelwood kinetic model. The catalytic reaction was carried out on the surface of the Pd NPs. As shown in Scheme 1, the 4-NP and hydrogen produced by hydrolysis of borohydride are first adsorbed on the surface of the catalyst. Electron transport and atom exchange were then carried out on the surface of the catalyst to produce the intermediate 4-Hx.<sup>54</sup> Finally, 4-Hx was reduced to the product 4-AP. The 4-AP was then released from the surface of the catalyst. The vacant active sites continue to be occupied by the reactants.

Fig. 8a-c showed the relationship between  $\ln(C_t/C_0)$  and time in our reaction was linear.  $C_t$  and  $C_0$  are the concentration of the 4-NP at reaction time  $t$  and initial time, respectively. The catalytic reduction of 4-NP was a pseudo-first-order reaction. This is because the concentration of NaBH<sub>4</sub> was very high and could be considered as a constant during our reaction.<sup>55</sup> The apparent rate constant  $k_{app}$  can be obtained from equation (1).

$$\ln \frac{C_t}{C_0} = \ln \frac{A_t}{A_0} = -k_{app} t \quad (1)$$

As shown in Fig. 8d, the relationship between apparent rate constants  $k_{app}$  and the amounts of Pd<sub>n</sub>-JP NPs was linear. This was due to an increase of the active site of Pd<sub>n</sub>-JP. Here, two important parameters were introduced to compare the catalytic performance of the catalyst. They are normalized rate constant ( $k_{nor} = k_{app}/c_{(Pd)}$ )<sup>56</sup> and turnover frequency (TOF). The TOF is defined as the number of moles of 4-NP reduced by per mole of catalyst per hour.<sup>8</sup> Pd<sub>50</sub>-JP had the highest  $k_{nor}$  and TOF in the Pd<sub>n</sub>-JP. The  $k_{nor}$  and TOF of Pd<sub>50</sub>-JP (1.0 nM) were calculated to be 38.4 s<sup>-1</sup>mM<sup>-1</sup> and 4455 h<sup>-1</sup>, respectively. More importantly, after one month, the  $k_{nor}$  and TOF of Pd<sub>50</sub>-JP (1.0 nM) were still as high as 37.3 s<sup>-1</sup>mM<sup>-1</sup> and 4334 h<sup>-1</sup>, indicating that the catalytic activity kept a long time. Table 1 showed

$k_{\text{nor}}$  and TOF of the Pd<sub>50</sub>-JP NPs and other catalyst reported in the literature.<sup>56-60</sup> The results revealed that Pd<sub>50</sub>-JP NPs had the highest  $k_{\text{nor}}$  and TOF, indicating they had the highest activity. The high catalytic performance of Pd<sub>n</sub>-JP NPs should depend on the small particle size of Pd NPs and high stability of Pd<sub>n</sub>-JP NPs in aqueous solution. Small particle size of Pd NPs typically had large specific surface areas and more active sites.<sup>61</sup> In addition, the high stability of Pd<sub>n</sub>-JP NPs in aqueous solution facilitated the rapid adsorption and release of the reactants, improving the effective contact between the reactants and the catalytically active sites. Therefore, Pd<sub>n</sub>-JP NPs had excellent catalytic activity.



**Fig. 8** The relationship between  $\ln(C_t/C_0)$  and the reaction time at 400 nm (a) Pd<sub>50</sub>-JP, (b) Pd<sub>100</sub>-JP, (c) Pd<sub>200</sub>-JP. (d) The relationship between  $k_{\text{app}}$  and concentration of Pd<sub>n</sub>-JP catalyst was linear. The results indicated that this catalytic reaction followed first-order kinetics and  $k_{\text{app}}$  increased with increasing active site of Pd<sub>n</sub>-JP.

**Table 1** Comparison of  $k_{\text{nor}}$  and TOF of Pd<sub>50</sub>-JP in this work and previously reported Pd-based catalysts for 4-NP reduction.

Catalyst	$k_{\text{nor}}(\text{s}^{-1}\text{mM}^{-1})$	TOF( $\text{h}^{-1}$ )	Reference
Pd/Fe <sub>3</sub> O <sub>4</sub> @SiO <sub>2</sub> @KCC-1	2.78	-	56
PdP/CNSs	1.4	504	57
Pd/CNSs	0.425	158	57
Pd/SBA-15	0.118	-	58
SPB/Pd	-	819	59
@Pd/CeO <sub>2</sub>	-	1068	60
Pd <sub>50</sub> -JP	38.4	4455	This work
Pd <sub>50</sub> -JP after one month	37.3	4334	This work

## 4 Conclusions

In conclusion, Pd<sub>n</sub>-JP NPs were synthesized using a green method, where JP was used as a reducing agent and stabilizer. The prepared Pd<sub>n</sub>-JP NPs were small, monodisperse, stable and biocompatible *in vitro*. Pd<sub>50</sub>-JP had the highest  $k_{\text{nor}}$  and TOF in the Pd<sub>n</sub>-JP and previously reported in the literature. It is worth noting that after

standing for one month, the  $k_{\text{nor}}$  and TOF of Pd<sub>50</sub>-JP (1.0 nM) were still as high as 37.3 s<sup>-1</sup>mM<sup>-1</sup> and 4334 h<sup>-1</sup>. This synthesis method is simple, green, it does not require the use of any external reducing agent. The prepared Pd<sub>n</sub>-JP NPs can be used in various bio-related application in the future.

## Acknowledgements

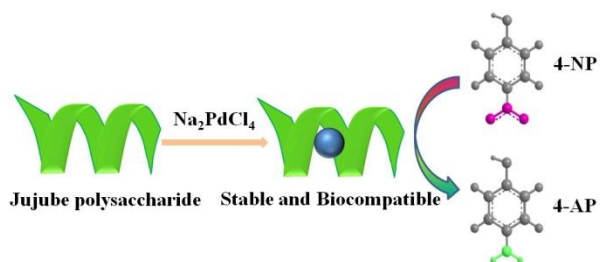
The authors appreciate financial support from the National Nature Science Foundation of China (21474085 and 21674092), the national development project on key basic research (973 Project, 2015CB655303), Natural Science Foundation of Hebei Province (B2017203229), Youth Foundation Project supported by the Hebei Education Department of China (QN2015034), China Postdoctoral Science Foundation (2016M601284), Postdoctoral Science Foundation of Hebei Province (B2016003017).

## Notes and references

- W. Shen, Y. Qu, X. Pei, S. Li, S. You, J. Wang, Z. Zhang and J. Zhou, *J. Hazard. Mater.*, 2017, 321, 299-306.
- Y. Li, Y. Cao, J. Xie, D. Jia, H. Qin and Z. Liang, *Catal. Commun.*, 2015, 58, 21-25.
- P. Deka, R. C. Deka and P. Bharali, *New J. Chem.*, 2014, 38, 1789-1793.
- M. Guo, J. He, Y. Li, S. Ma and X. Sun, *J. Hazard. Mater.*, 2016, 310, 89-97.
- Z. Dong, X. Le, C. Dong, W. Zhang, X. Li and J. Ma, *Appl. Catal., B*, 2015, 162, 372-380.
- P. S. Rajegaonkar, B. A. Deshpande, M. S. More, S. S. Waghmare, V. V. Sangawe, A. Inamdar, M. D. Shirsat and N. N. Adhasure, *Mater. Sci. Eng., C*, 2018, 93, 623-629.
- T. Ma, W. Yang, S. Liu, H. Zhang and F. Liang, *Catalysts*, 2017, 7, 38.
- L. Wang, Q. Yang, Y. Cui, D. Gao, J. Kang, H. Sun, L. Zhu and S. Chen, *New J. Chem.*, 2017, 41, 8399-8406.
- S. Lebaschi, M. Hekmati and H. Veisi, *J. Colloid Interface Sci.*, 2017, 485, 223-231.
- X. Qiao, Z. Zhang, F. Tian, D. Hou, Z. Tian, D. Li and Q. Zhang, *Cryst. Growth Des.*, 2017, 17, 3538-3547.
- W. Tseng, C. Lee and W. Tseng, *ACS App. Nano Mater.*, 2018, 1, 6808-6817.
- S. Liu, A. Qileng, J. Huang, Q. Gao and Y. Liu, *RSC Adv.*, 2017, 7, 45545-45551.
- S. Gu, S. Wunder, Y. Lu, M. Ballauff, R. Fenger, K. Rademann, B. Jaquet and A. Zacccone, *J. Phys. Chem. C*, 2014, 118, 18618-18625.
- S. Gu, Y. Lu, J. Kaiser, M. Albrecht, M. B. Phys. Chem. Chem. Phys., 17 (2015) 28137-28143.
- A. R. Abbasi, H. Kalantary, M. Yousefi, A. Ramazani and A. Morsali, *Ultrason. Sonochem.*, 2012, 19, 853-857.
- K. Tahir, B. Li, S. Khan, S. Nazir, Z. U. Haq Khan, A. U. Khan and R. U. Islam, *J. Alloys Compd.*, 2015, 651, 322-327.
- A. K. Vala, *Environ. Prog. Sustain.*, 2015, 34, 194-197.
- P. Rauwel, S. K. Üinal, S. Ferdov and E. Rauwel, *Adv. Mater. Sci. Eng.*, 2015, 2015, 1-9.
- S. P. Chandran, M. Chaudhary, R. Pasricha, A. Ahmad, M. Sastry, *Biotechnol. Progr.*, 2006, 22, 577-583.
- A. Saxena, R. M. Tripathi, F. Zafar and P. Singh, *Mater. Lett.*, 2012, 67, 91-94.

- 21 M. Nasrollahzadeh, S. M. Sajadi, A. Rostami-Vartooni, M. Bagherzadeh and R. Safari, *J. Mol. Catal. A: Chem.*, 2015, 400, 22-30.
- 22 D. MubarakAli, N. Thajuddin, K. Jeganathan and M. Gunasekaran, *Colloids Surf., B*, 2011, 85, 360-365.
- 23 J. Yu, D. Xu, H. N. Guan, C. Wang, L. K. Huang and D. F. Chi, *Mater. Lett.*, 2016, 166, 110-112.
- 24 P. Patra, D. Das, B. Behera, T. K. Maiti and S. S. Islam, *Carbohydr. Polym.*, 2012, 87, 2169-2175.
- 25 S. Saha, M. H. Navid, S. S. Bandyopadhyay, P. Schnitzler and B. Ray, *Carbohydr. Polym.*, 2012, 87, 123-130.
- 26 M. Zou, Y. Chen, D. Sun-Waterhouse, Y. Zhang and F. Li, *Food Chem.*, 2018, 258, 35-42.
- 27 T. L. Bray, M. Salji, A. Brombin, A. M. Pérez-López, B. Rubio-Ruiz, L. C. A. Galbraith, E. E. Patton, H. Y. Leung and A. Unciti-Broceta, *Chem. Sci.*, 2018, 9, 7354-7361.
- 28 M. A. Miller, B. Askevold, H. Mikula, R. H. Kohler, D. Pirovich and R. Weissleder, *Nat. Commun.*, 2017, 8, 15906.
- 29 K. Esumi, R. Isono and T. Yoshimura, *Langmuir*, 2004, 20, 237-243.
- 30 J. Chen, S. Tian, X. Shu, H. Du, N. Li and J. Wang, *Int. J. Mol. Sci.*, 2016, 17, 1011.
- 31 V. Samavati and A. Manoochehrizade, *Int. J. Biol. Macromol.*, 2013, 60, 427-436.
- 32 J. Li, Y. Liu, L. Fan, L. Ai and L. Shan, *Carbohydr. Polym.*, 2011, 84, 390-394.
- 33 C. Gao, Y. Wang, C. Wang and Z. Wang, *Carbohydr. Polym.*, 2013, 92, 2187-2192.
- 34 L. Wang, Y. Cui, S. Chen, G. Wang, D. Gao, Y. Liu, Q. Luo, Z. Liu and X. Zhang, *Mater. Sci. Eng., C*, 2017, 78, 315-323.
- 35 Y. He, M. Yang, S. Zhao, C. Cong, X. Li, X. Cheng, J. Yang and D. Gao, *ACS Sustain. Chem. Eng.*, 2018, 6, 13543-13550.
- 36 X. Liu, Q. Jin, Y. Ji and J. Ji, *J. Mater. Chem.*, 2012, 22, 1916-1927.
- 37 X. Zhang, L. Luo, L. Li, Y. He, W. Cao, H. Liu, K. Niu and D. Gao, *Nanomedicine*, 2019, 15, 142-152.
- 38 A. I. Lopez, R. Y. Reins, A. M. McDermott, B. W. Trautner and C. Cai, *Mol. Biosyst.*, 2009, 5, 1148-1156.
- 39 A. Raza, F. Li, X. Xu and J. Tang, *Int. J. Biol. Macromol.*, 2017, 94, 335-344.
- 40 J. Wu, P. Li, D. Tao, H. Zhao, R. Sun, F. Ma and B. Zhang, *Int. J. Biol. Macromol.*, 2018, 117, 1299-1304.
- 41 X. Wu, C. Lu, W. Zhang, G. Yuan, R. Xiong and X. Zhang, *J. Mater. Chem. A.*, 2013, 1, 8645-8652.
- 42 S. S. A. Darbandizadeh Mohammad Abadi and M. A. Karimi Zarchi, *New J. Chem.*, 2017, 41, 10397-10406.
- 43 A. Santoshi kumari, M. Venkatesham, D. Ayodhya and G. Veerabhadram, *Appl. Nanosci.*, 2014, 5, 315-320.
- 44 S. Maity, I. Kumar Sen and S. Sirajul Islam, *Physica E*, 2012, 45, 130-134.
- 45 M. V. Sujitha and S. Kannan, *Spectrochim. Acta, Part. A*, 2013, 102, 15-23.
- 46 J. Baharara, F. Namvar, T. Ramezani, N. Hosseini and R. Mohamad, *Molecules*, 2014, 19, 4624-4634.
- 47 L. Wang, J. Zhang, X. Guo, S. Chen, Y. Cui, Q. Yu, L. Yang, H. Sun, D. Gao and D. Xie, *New J. Chem.*, 2018, 42, 19740-19748.
- 48 Y. Cui, B. Liang, L. Wang, L. Zhu, J. Kang, H. Sun and S. Chen, *Mater. Sci. Eng., C*, 2018, 93, 332-340.
- 49 K. Liu, L. Han, J. Zhuang and D. P. Yang, *Mater. Sci. Eng., C*, 2017, 78, 429-434.
- 50 S. Gu, J. Kaiser, G. Marzun, A. Ott, Y. Lu, M. Ballauff, A. Zacccone, S. Barcikowski and P. Wagener, *Catalysis Letters*, 2015, 145, 1105-1112.
- 51 S. Panigrahi, S. Basu, S. Praharaj, S. Pande, S. Jana, A. Pal, S. K. Ghosh, T. Pal, *J. Phys. Chem. C*, 2007, 111, 4596-4605.
- 52 K. B. Narayanan and N. Sakthivel, *J. Hazard. Mater.*, 2011, 189, 519-525. View Article Online  
DOI: 10.1039/C9NJ00950G
- 53 R. Begum, R. Rehan, Z. H. Farooqi, Z. Butt and S. Ashraf, *J. Neurosci. Res.*, 2016, 18, 231.
- 54 S. Harish, J. Mathiyarasu, K. L. N. Phani and V. Yegnaraman, *Catal. Lett.*, 2008, 128, 197-202.
- 55 Z. Dong, X. Le, X. Li, W. Zhang, C. Dong and J. Ma, *Appl. Catal., B*, 2014, 158-159, 129-135.
- 56 X. Le, Z. Dong, Y. Liu, Z. Jin, T.-D. Huy, M. Le and J. Ma, *J. Mater. Chem. A*, 2014, 2, 19696-19706.
- 57 Z. Zhao, X. Ma, X. Wang, Y. Ma, C. Liu, H. Hang, Y. Zhang, Y. Du and W. Ye, *Appl. Surf. Sci.*, 2018, 457, 1009-1017.
- 58 J. Morère, M. J. Tenorio, M. J. Torralvo, C. Pando, J. A. R. Renuncio and A. Cabañas, *J. Supercrit. Fluids.*, 2011, 56, 213-222.
- 59 Y. Mei, Y. Lu, F. Polzer, M. Ballauff, *Chem. Mater.*, 2007, 19, 1062-1069.
- 60 B. Liu, S. Yu, Q. Wang, W. Hu, P. Jing, Y. Liu, W. Jia, Y. Liu, L. Liu and J. Zhang, *Chem. Commun.*, 2013, 49, 3757-3759.
- 61 W. Chen, Z. Zhu and L. Yang, *Int. J. Hydrogen Energy*, 2017, 42, 24404-24411.

## 1. TOC

View Article Online  
DOI: 10.1039/C9NJ00950G

2. Jujube polysaccharide-stabilized palladium nanoparticles provide active sites for efficient catalysis of 4-nitrophenol to 4-aminophenol.